

## Self-Assembly of Normal Alkanes on the Au (111) Surfaces

Hai-Ming Zhang, Zhao-Xiong Xie,\* Bing-Wei Mao, and Xin Xu\*[a]

**Abstract:** The self-assembled monolayers (SAMs) of normal alkanes ( $n\text{-C}_n\text{H}_{2n+2}$ ) with different carbon chain lengths ( $n=14\text{--}38$ ) in the interfaces between alkane solutions (or liquids), and the reconstructed Au (111) surfaces have been systematically studied by means of scanning tunneling microscopy (STM). In contrast to previous studies, which concluded that some  $n$ -alkanes ( $n=18\text{--}26$ ) can not form well-ordered structures on Au (111) surfaces, we observed SAM formations for all these  $n$ -alkanes without any exceptions. We find that gold reconstruc-

tion plays a critical role in the SAM formation. The alkane monolayers adopt a lamellar structure in which the alkane molecules are packed side-by-side, to form commensurate structures with respect to the reconstructed Au (111) surfaces. The carbon skeletons are found to lie flat on the surfaces, which is consistent with the infrared spectroscopic studies. Interestingly, we

find that two-dimensional chiral lamellar structures form for alkanes with an even carbon number due to the specific packing of alkane molecules in a tilted lamella. Furthermore, we find that the orientation of alkane molecules deviates from the exact  $[01\bar{1}]$  direction, because of the intermolecular interactions among the terminal methyl groups of neighboring lamellae; this results in differences of molecular orientation between mirror structures of adjacent zigzag alkane lamellae. Structural models have been proposed, that shed new light on monolayer formation.

**Keywords:** alkanes • gold • physisorption • scanning probe microscopy • self-assembly

### Introduction

Self-assembled monolayers (SAMs) at the interfaces between a metal and an organic solution have attracted widespread interest, because of the importance for potential applications in many fields such as lubrication, sensors, corrosion protection, and chemical reactions. Although a well-ordered molecular layer on a single-crystal surface can provide a template in molecular level engineering,<sup>[1]</sup> fundamental problems such as the origin of the self-assembly phenomena should be understood before this technique can be applied in the fields of nanotechnology.

As a representative class of physisorbed systems, self-assembly of normal alkanes ( $n$ -alkanes,  $\text{C}_n\text{H}_{2n+2}$ ) on solid surfaces has been studied intensively by means of low energy electron diffraction (LEED), infrared spectroscopy (IR), scanning tunneling microscopy (STM), and molecular dynamics simulation.<sup>[2–13]</sup> STM studies have provided unprece-

ded structural details about physisorbed alkanes. Earlier studies are mainly focused on the self-assembly of alkanes on highly oriented pyrolytic graphite (HOPG) surfaces.<sup>[7–9]</sup> STM studies of alkanes self-assembly on metal surfaces have appeared only recently.<sup>[14–22]</sup> Uosaki et al. first reported the formation of self-organized  $n$ -alkanes on Au (111) surfaces in neat liquid by in situ STM.<sup>[14,15]</sup> It was further understood that gold reconstruction plays a critical role in the formation of well-ordered structures, as reported in our previous paper.<sup>[16]</sup> Very recently it was reported by He et al., that the electrochemical potential induced self-assembly of hexadecane on Au(111) in the aqueous solution, by using electrochemical scanning tunneling microscopy.<sup>[23]</sup> Although the self-assembly of  $n$ -alkanes on Au (111) surfaces has been explored by several groups, so far, there is no systematic interpretation on this phenomenon; this might be due to insufficient experimental data, especially for the structures of alkanes with different chain lengths.

In this paper, we present systematic studies of the self-assembly of  $n$ -alkanes,  $\text{C}_n\text{H}_{2n+2}$ ,  $n$  from 14 to 38. Despite earlier studies, which concluded some  $n$ -alkanes ( $n$  from 18 to 26) can not form well-ordered structures on Au (111) surfaces,<sup>[17,21,22]</sup> we have successfully observed SAM formations of these alkanes. Based on our systematic high-resolution STM images, the self-assembly phenomena of  $n$ -alkanes on the Au(111) surfaces are discussed, and shed new light on monolayer formation.

[a] H.-M. Zhang, Prof. Dr. Z.-X. Xie, Prof. Dr. B.-W. Mao, Prof. Dr. X. Xu  
State Key Laboratory of Physical Chemistry  
of Solid Surfaces, Department of Chemistry  
Xiamen University, Xiamen 361005 (China)  
Fax: (+86) 592-218-3047  
E-mail: zxxie@xmu.edu.cn  
xinxu@xmu.edu.cn

## Experimental Section

Reconstructed Au (111) surfaces of a single-crystalline bead fixed on a Au sheet were prepared by the Clavilier's method,<sup>[24]</sup> followed by careful annealing in a hydrogen flame. Saturated solutions of *n*-alkanes from *n*-eicosane ( $n\text{C}_{20}\text{H}_{42}$ ) to *n*-octacosane ( $n\text{C}_{28}\text{H}_{58}$ ), and *n*-triacontane ( $n\text{C}_{30}\text{H}_{62}$ ), *n*-tritriacontane ( $n\text{C}_{33}\text{H}_{68}$ ), *n*-hexatriacontane ( $n\text{C}_{36}\text{H}_{74}$ ). Also, *n*-octatriacontane ( $n\text{C}_{38}\text{H}_{78}$ ) in *n*-tetradecane ( $n\text{C}_{14}\text{H}_{30}$ ) (99 %, Alfa) were used, while for *n*-tetradecane ( $n\text{C}_{14}\text{H}_{30}$ ), *n*-hexadecane ( $n\text{C}_{16}\text{H}_{34}$ , 98 % Sigma) we used neat liquids, and for *n*-octadecane ( $n\text{C}_{18}\text{H}_{38}$ ) we used a 50 % solution from the solvent of *n*-tetradecane ( $n\text{C}_{14}\text{H}_{30}$ ). After putting an alkane solution or an alkane neat liquid on the freshly annealed Au (111) surface, a mechanically sharpened Pt/Ir tip was immersed in for STM observation (Nanoscope IIIa, Digital Instrument) at room temperature (25 °C). To obtain good images for *n*-tetradecane ( $n\text{C}_{14}\text{H}_{30}$ ), the STM observations were carried out at 20 °C. Typical imaging conditions included a bias voltage of 100 mV, and a tunneling current of 1.5 nA.

## Results and Discussion

### Self-assembly of *n*-alkanes at the interfaces between alkane liquids/solutions, and reconstructed Au (111) surfaces from $n\text{C}_{14}\text{H}_{30}$ to $n\text{C}_{38}\text{H}_{78}$ :

The STM studies for the self-assembly phenomena of *n*-alkanes ( $n\text{C}_n\text{H}_{2n+2}$ ) at the interfaces between alkane solution and reconstructed Au(111) surfaces have been reported by several groups.<sup>[14–22]</sup> Both alkanes with odd *n* and even *n* (hereafter, odd alkanes and even alkanes, respectively) have been studied.<sup>[14–22]</sup> Some earlier studies concluded that no ordered monolayer can be formed with *n* from 18 to 26.<sup>[17,21,22]</sup>

Figure 1 shows typical STM images of *n*-alkane monolayers on the reconstructed Au(111) surfaces. Figure 1b, c, e, f, and h show images for the even alkanes from *n* = 18 to 26. The STM images of  $n\text{C}_{14}\text{H}_{30}$  (Figure 1a and  $n\text{C}_n\text{H}_{2n+2}$  (*n* = 28, 30, 38 in i, j, and l), respectively) are shown as representative images for *n* < 18 and *n* > 26 for the even alkanes. For the odd alkanes, the STM images for the self-assembled monolayers of  $n\text{C}_{21}\text{H}_{43}$ ,  $n\text{C}_{25}\text{H}_{52}$ , and  $n\text{C}_{33}\text{H}_{68}$  are presented as examples (see Figure 1d, g, and k). As can be clearly seen from Figure 1, superimposed lamellar structures are formed on the reconstructed Au(111) surfaces, in which the typical reconstruction ridges can be well identified. Every lamella is composed of close-packed rods. The length of each rod is very consistent to the length of an alkane molecule. Each rod in the lamellae is then considered as an individual alkane molecule. Furthermore, no ordered alkane monolayer can be observed on the unreconstructed Au(111) surfaces at the same condition, as pointed out in our previous paper.<sup>[16]</sup> Thus we conclude that self-assembly of *n*-alkanes ( $n\text{C}_n\text{H}_{2n+2}$ , *n* = 14–38) can be formed on the reconstructed Au(111) surfaces with no exception.

Marchenko and Cousty proposed a model, in which the carbon skeleton plane of an alkane was assumed to be perpendicular to Au(111).<sup>[17]</sup> They deduced that the geometric mismatch between the periodicity of gold (interatomic distance 0.288 nm neglecting the reconstruction of gold), and the two-neighboring  $\text{CH}_2$  groups (0.251 nm) causes oscillation of adsorption energy with an increase in carbon chain number. They then concluded that no ordered molecular structure could be detected from  $n\text{C}_{18}\text{H}_{38}$  to  $n\text{C}_{26}\text{H}_{54}$ .<sup>[17,21,22]</sup>

We believe that alkanes adsorb on the Au(111) surfaces with their skeleton planes being parallel to Au(111). The structures of the monolayers are determined by the competition between the adsorbate–substrate interaction, and the adsorbate–adsorbate interaction. The gold reconstruction plays a critical role in the formation of the well-ordered structures. A detailed discussion follows below.

### Influence of gold reconstruction ridges on the packing of alkane molecules:

Models for the reconstructed Au(111) surfaces are schematically illustrated in Figure 2. Figure 2a shows a uniaxial (straight) reconstructed surface, in which the lattice shortening occurs along the  $[1\bar{1}0]$  direction, such that 23 Au atoms are packed in the space of 22 original Au atoms. Notice that the contraction of the surface atoms is anisotropic. Thus the periodicity of the reconstructed Au lattice remains the same value of 0.5 nm as that in the unreconstructed Au(111) along the direction of  $[11\bar{2}]$ , and the periodicity is reduced to 0.48 nm along the direction of  $[\bar{2}11]$  or  $[1\bar{2}1]$ . In this model, the gold reconstruction ridges are along the  $[11\bar{2}]$  direction. The reconstructed Au(111) surfaces may exhibit a herringbone arrangement of (or V-shaped) ridges, as shown in Figure 2b. In this herringbone-like reconstructed surface, there exist two kinds of straight reconstructed domains that differ by 120°.

The well-identified gold reconstruction ridges in each STM image can be used to locate the arrangements of the alkane molecules. The long axes of alkane molecules are always measured to be around 30° with respect to the Au(111) reconstruction ridges. Here, we did not find the long axes of alkane molecules to be perpendicular to the Au(111) reconstruction ridges at room temperature (25 °C). Therefore, we deduce that the long axes of alkane molecules are along the  $[01\bar{1}]$  or  $[\bar{1}01]$  direction of the Au (111) substrate, and the long axes of alkane molecules will not locate along the  $[1\bar{1}0]$  direction; although the  $[1\bar{1}0]$  direction is equivalent to the  $[01\bar{1}]$  or  $[\bar{1}01]$  direction if the reconstruction is neglected (c.f. Figure 2). By measuring the intermolecular distances of alkane molecules along the  $[11\bar{2}]$  direction, we find that all the distances are close to the value of 0.48 nm. One must recall that alkane molecules adopt the intermolecular distance of 0.48 nm in their bulk crystals, and the periodicity of the reconstructed Au(111) along the direction of  $[211]$  or  $[1\bar{2}1]$  is again 0.48 nm, therefore we infer that the self-assembled alkane monolayers are commensurate with the reconstructed Au(111) surfaces, such that both adsorbate–adsorbate interactions, and adsorbate–substrate interactions are optimized.<sup>[25]</sup>

On the unreconstructed Au(111) surfaces or along the direction perpendicular to the gold reconstructed ridges, that is, along the  $[1\bar{1}0]$  direction in our model, the optimized adsorbate–adsorbate interactions and adsorbate–substrate interactions can not be reached. This is consistent with the fact that no well-ordered structure on the unreconstructed Au (111) surfaces can be observed, and alkane molecules do not preferentially orientate along the direction perpendicular to the gold reconstructed ridges at room temperature. However, in a very recent paper,<sup>[23]</sup> well-organized structures of alkanes on the unreconstructed Au (111) surfaces

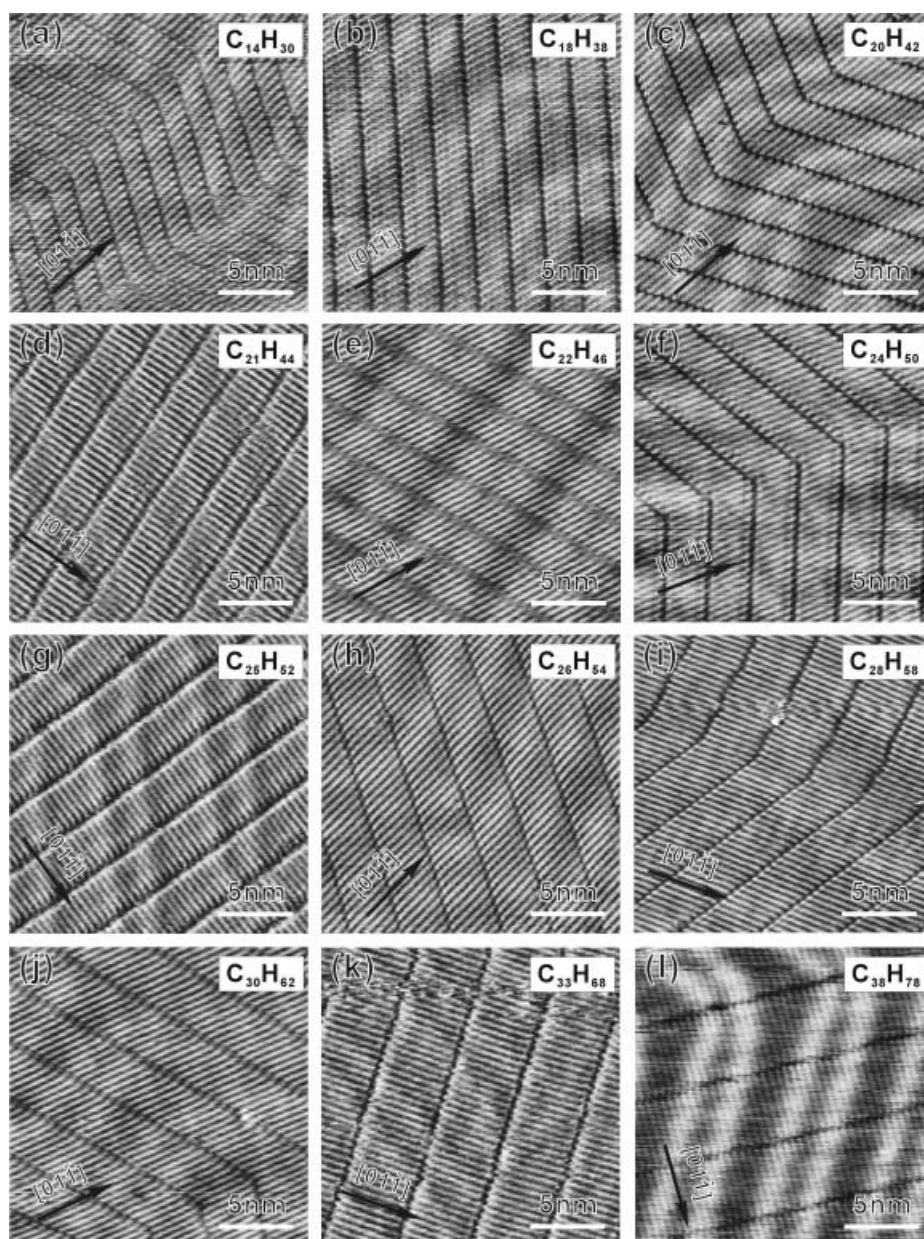


Figure 1. STM images of self-assembled  $n$ -alkanes (from  $n\text{C}_{14}\text{H}_{30}$  to  $n\text{C}_{38}\text{H}_{78}$ ) on the reconstructed Au (111) surfaces. Images from b) to h) exhibit the well-ordered structures of  $n$ -alkanes for  $n$  from 18 to 26, which were previously concluded as ‘absence of structure’.<sup>[17]</sup> Images a), i), j), and l) are from  $n\text{C}_{14}\text{H}_{30}$ ,  $n\text{C}_{28}\text{H}_{52}$ ,  $n\text{C}_{30}\text{H}_{62}$  and  $n\text{C}_{38}\text{H}_{78}$ , respectively, and show the representative alkanes for  $n < 18$  and  $n > 26$  with even  $n$ . Images d), g), and k) are representative for odd  $n$  with  $n = 21, 25, 33$ , respectively. Arrows on images label the  $[01\bar{1}]$  direction on Au(111) surfaces (c.f. Figure 2). All images are of  $20\text{ nm} \times 20\text{ nm}$  at the tunneling condition of  $V_t = 0.1\text{ V}$ ,  $I_t = 1.5\text{ nA}$ .

have been successfully obtained in aqueous solution under potential control by using electrochemical STM. Therefore, assisted by an external force, such as the electric field, such an unstable monolayer structure can be stabilized.

Surface corrugation further reduces the possibility for alkanes to adsorb along the  $[1\bar{1}0]$  direction. Wöll et al. showed that the fcc (face cubic center) and hcp (hexagonal closed packing) stacking regions are connected by partial Shockley dislocations with Burgers vector  $\frac{1}{6}(1,1,-2)$ .<sup>[26]</sup> The displacement of the atoms from the straight line drawn

along the  $[1\bar{1}0]$  direction can be up to  $0.7\text{ \AA}$ , which makes it unfeasible for alkanes to adsorb along this direction.

In our previous paper,<sup>[16,20]</sup> it was found that there is a slight difference in the orientation of the molecular axis between two sides of the elbow position of the herringbone reconstruction ridges. By checking all available STM images, we conclude that such slightly different orientations of alkane molecules in different sides of the herringbone elbow position exist in all alkane monolayers. Figure 3 shows examples of such phenomena for different alkanes, in which

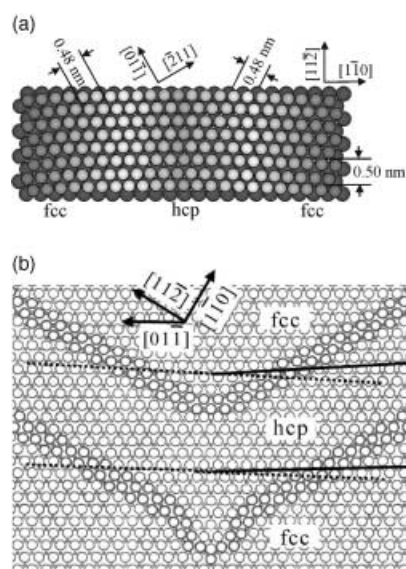


Figure 2. The schematic models of the reconstructed Au (111) surfaces. a) The uniaxial reconstructed surface. The lattice shortening occurs along the  $[01\bar{1}]$  direction where 23 Au atoms are packed in a space of the 22 original Au atoms. b) The reconstruction with herringbone-like (V-shape) ridges. The solid and dashed lines show the slight difference of the gold troughs between the different sides of the V-shape ridges along the about  $[01\bar{1}]$  direction.

the orientation of alkane molecules are marked on the figures with dashed and solid lines in the different sides of the elbow position of the herringbone reconstruction ridges. The deviation angles are measured around  $2^\circ$ – $3^\circ$ .

As pointed out in our previous paper,<sup>[16,20]</sup> the structures of the alkane monolayers are perturbed by the herringbone reconstruction ridges underneath them. The model in Figure 2b clearly shows that there is a slightly different orientation of the gold troughs along the approximate  $[01\bar{1}]$  direction on both sides of the reconstructed ridges. This deviation results from the different transition structures from the fcc position to the hcp position, and from hcp to fcc positions. The theoretical average deviation angle is about  $2.6^\circ$ . By considering the structures of the Au (111) reconstructed surfaces, it is reasonable to deduce that the alkane molecules adsorb along the gold troughs, in which each alkane molecule interacts with two neighboring rows of gold atoms

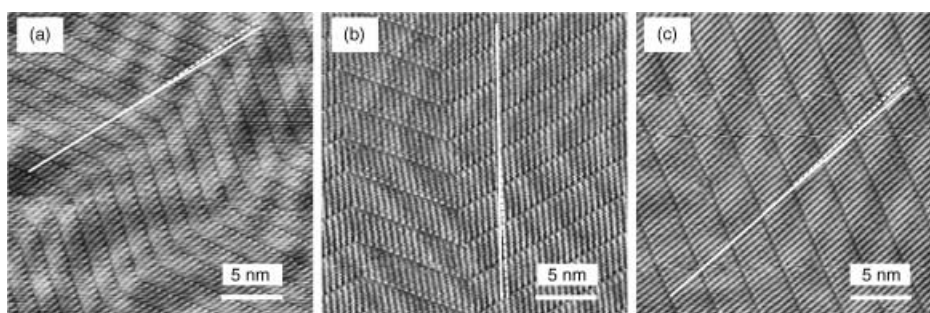


Figure 3. STM images of the self-assembled monolayers formed by a)  $nC_{14}H_{30}$ , b)  $nC_{20}H_{42}$  and c)  $nC_{26}H_{54}$ . The solid and dash lines show the slight difference in the orientation of the molecular axes between two sides of the elbow position of the herringbone reconstruction ridges. The deviation angles are around  $2^\circ$ – $3^\circ$ .

along the  $[01\bar{1}]$  direction, such that a commensurate structure is developed between an alkane monolayer and the gold reconstructed surface. Therefore, the small deviation in gold rows results in a small orientation difference of the adsorbed alkane molecules.

Two kinds of lamellar structures can be identified from the STM images of the self-assembled alkane monolayers (Figure 1). The long axes of the alkane molecules can be either perpendicular or tilted to the lamellar boundaries. To simplify the description of these two kinds of lamellar structures, we will call the former perpendicular lamellae, and the latter tilted lamellae. For the monolayers of odd alkanes, only perpendicular lamellae are observed, while for the monolayers of even alkanes, both perpendicular and tilted lamellae can be observed (See Figure 1). The lamellar structures are found to be sensitive to the length of the carbon chain for the even alkanes. At room temperature ( $25^\circ\text{C}$ ), the long axes of alkane molecules are always found to be tilted to the lamellar boundary if  $n < 22$ . Perpendicular lamellae appear in the self-assembled monolayer of  $n$ -docosane ( $nC_{22}H_{46}$ ) at room temperature, although tilted lamellae dominate as shown in Figure 4a. Tilted and perpendicular lamellae coexist in the monolayers even for alkane  $n \geq 22$ , while the percentage of the perpendicular lamellae increase as  $n$  increases. In fact, in the monolayer of  $n$ -octatriacontane ( $nC_{38}H_{78}$ ), very few tilted lamellae can be found on the herringbone-like gold surfaces, as shown in Figure 4b.

We emphasize that the observed lamellar structures should be attributed to a combined effect of the adsorbate–

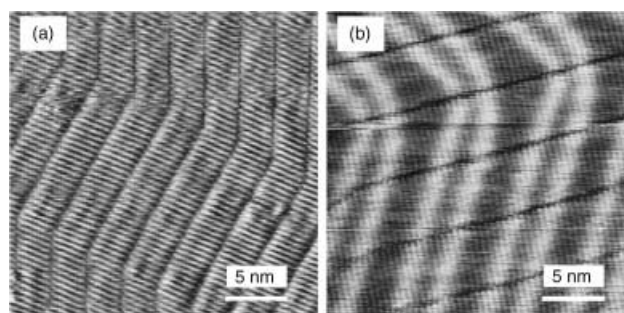


Figure 4. a) STM image of  $nC_{22}H_{46}$  at room temperature, showing the coexistence of tilted lamellae and perpendicular lamellae. b) STM image of  $nC_{38}H_{78}$  at room temperature, in which few tilted lamellae can be found.

adsorbate interactions and the adsorbate–substrate interactions. Based on the adsorbate–adsorbate interactions, to form a close packed structure, Uosaki and co-workers showed that odd alkanes adopt the perpendicular lamellar structure regardless of the carbon number, while both perpendicular and tilted lamellae are possible for even alkanes.<sup>[15]</sup> They concluded that this odd/even effect arises from the difference in the symmetry of the molecule, which is determined by the direction of the terminal methyl groups. For odd alkanes, Uosaki et al. inferred that the stability of the alkane monolayer is enhanced by the adsorbate–substrate interaction when a perpendicular lamellar structure is adopted, in this way; the alkane monolayer possesses a common symmetric axis with the gold substrate.<sup>[15]</sup> For even alkanes, our previous calculations based on the molecular mechanism suggested that tilted lamellae (with the neighboring alkane molecule shifting in one repeated unit of methylene group) have a slight energetic preference if the adsorbate–substrate interactions are neglected.<sup>[19]</sup>

We postulate that the adsorbate–substrate interactions strongly influence the lamellar structures of the even alkanes. A strong adsorbate–substrate interaction favors the perpendicular lamellae, while a tilted lamella is preferable if the adsorbate–substrate interaction is weak. This hypothesis is supported by the fact that perpendicular lamellae were always observed on HOPG,<sup>[7–9]</sup> and only tilted lamellae were detected on the basal plane of MoS<sub>2</sub> plane,<sup>[10,11,27]</sup> while the heat of adsorption for *n*-dotriacontane (*n*C<sub>32</sub>H<sub>66</sub>) on MoS<sub>2</sub> was measured to be approximately 1/3 of the value obtained on graphite.<sup>[28]</sup> We deduce that the alkane–gold interaction is in between the alkane–HOPG, and the alkane–MoS<sub>2</sub> interactions is such that both perpendicular and tilted lamellae are observed for  $38 > n \geq 22$  at room temperature. The alkane–gold interaction increases with an increase in carbon chain length, hence the perpendicular lamellae dominate for  $n \geq 38$ , whereas the tilted lamellae prevail for  $n < 22$ .

Helium atom reflectivity has been used to study the adsorption of a series of *n*-alkanes on Au(111) surfaces.<sup>[29]</sup> For *n*-alkanes up to C<sub>12</sub>H<sub>26</sub>, it was found that the adsorption energy increases linearly with the chain length by 6.2 kJ mol<sup>-1</sup> per additional methylene unit ( $n=6$ ), while there is a 19.0 kJ mol<sup>-1</sup> zero offset arising in part from differences between the methyl and methylene subunits.<sup>[30]</sup> Based on the bond additive model,<sup>[29]</sup> we deduce that the adsorption energy is around 155.4 kJ mol<sup>-1</sup> for C<sub>22</sub>H<sub>46</sub> on Au(111). This may be compared to the measured desorption barrier of 166.2 kJ mol<sup>-1</sup> for C<sub>22</sub>H<sub>46</sub> adsorbed on HOPG,<sup>[30]</sup> which lends support to the idea that the alkane–gold interaction would be weaker than the alkane–HOPG interaction.

#### Molecular packing in the lamellae of alkane monolayer:

Vacuum-deposited films of *n*C<sub>44</sub>H<sub>90</sub> on a Au(111) surface have been investigated by infrared reflection absorption spectroscopy. A flat-on structure was found to be formed by molecules in an all-*trans* conformation with the carbon skeleton parallel to the surface for the first monolayer physisorbed on the surface.<sup>[4]</sup> Early LEED studies of light alkanes (C<sub>3</sub>–C<sub>8</sub>) on Pt(111) and Ag(111) surfaces advocate the same flat-on structure. High-resolution STM images may not

show every methylene group of an alkane molecule. For example, Cousty and Marchenko showed that the STM image of a *n*C<sub>16</sub>H<sub>34</sub> molecule corresponds to 8 bumps when adsorbed on gold, and thus concluded that carbon skeletons of the adsorbed alkanes are perpendicular to Au(111).<sup>[22]</sup>

To resolve this controversy, various kinds of tunneling conditions are applied. Figure 5 shows the STM images of

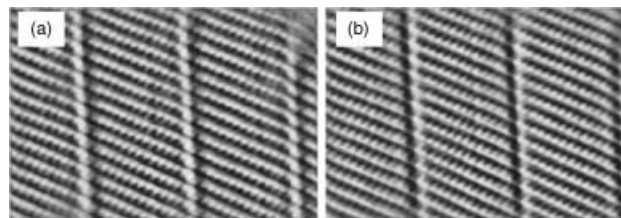


Figure 5. STM images of *n*C<sub>28</sub>H<sub>58</sub> recorded in the same area with tip direction from right to left (retrace a) and left to right (trace b). Scanning size: 10 nm × 7 nm; constant height mode.

*n*C<sub>28</sub>H<sub>58</sub>, in which bright spots with half of the carbon number were observed. With the constant height mode, we recorded both ‘retrace’ (tip scanning from right to left) and ‘trace’ (tip scanning from left to right) images at the same area, as shown in Figure 5a and b, respectively. Interestingly, we find that brighter spots appear in the left side of the alkane molecules when the STM tip is scanned from left to right, while the right side of the molecules become brighter when the tip is scanned from right to left. These results strongly suggest that these STM images do not directly reflect the surface relief, since such bright spots with  $n/2$  do not correspond to a vertical adsorption mode of C<sub>*n*</sub>H<sub>2*n*+2</sub> on the surfaces. Instead, the observation that left or right carbon atoms light up in ‘trace’ or ‘retrace’ images implies that the alkanes adopt a parallel adsorption mode on the surfaces. Figure 6a shows the STM image of *n*C<sub>28</sub>H<sub>58</sub> with constant current mode. Again, bright spots with half the number of carbon atoms were imaged. However, by only adjusting the long axes of the alkane molecules to be vertical to the STM tip scanning direction, the atomic resolution zigzag methylene groups on the alkane molecules were observed, as shown in Figure 6b. In other words, we find that full carbon atoms can be imaged only when the STM tip scanning direction is perpendicular to the long axes of the alkane molecules, otherwise only half of carbon atoms can be imaged. The scanning-direction dependence of the STM images is very reproducible, and appears on all the alkanes. Figure 6c shows another example, in which the zigzag methylene groups for *n*C<sub>22</sub>H<sub>46</sub> all show up by adjusting the molecules perpendicular to the scanning direction. Therefore, we conclude that alkanes adopt a flat-on structure when adsorbed on gold surfaces; this is in agreement with the infrared spectroscopy results,<sup>[4]</sup> and the LEED results.<sup>[2,3]</sup>

Marchenko and Cousty emphasized the importance of the geometric mismatch between the periodicity of gold (interatomic distance 0.288 nm neglecting the reconstruction of gold), and the two neighboring CH<sub>2</sub> groups (0.251 nm).<sup>[17]</sup> They concluded that it is this mismatch that causes the oscillation of the adsorption energy with carbon chain number,

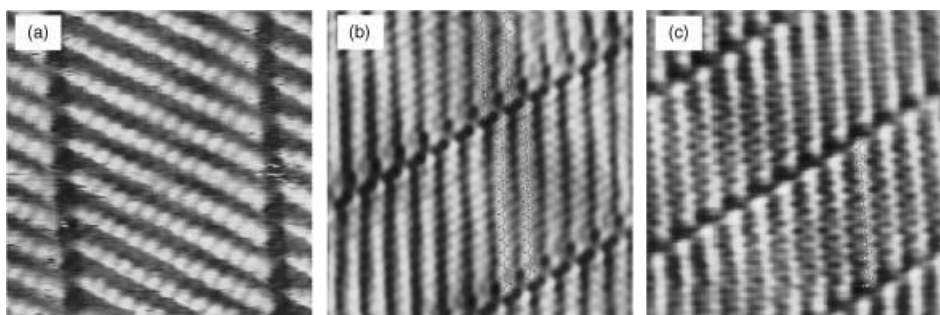


Figure 6. Tip scanning direction dependence of STM images, showing the different appearance of two atomic resolution images with different scanning direction. a) STM image of  $C_{28}H_{58}$  acquired with the tip scanning direction nonperpendicular to the molecular axes of alkanes (scan size:  $5\text{ nm} \times 5\text{ nm}$ ). b) STM image of  $C_{28}H_{58}$  with the tip scanning direction perpendicular to the molecular axes of alkanes (scan size:  $6\text{ nm} \times 6\text{ nm}$ ). c) STM image of  $C_{22}H_{46}$  with the tip scanning direction perpendicular to the molecular axes of alkanes (scan size:  $6\text{ nm} \times 6\text{ nm}$ ).

such that, no ordered molecular-structure could be detected from  $nC_{18}H_{38}$  to  $nC_{26}H_{54}$ .<sup>[17,21,22]</sup> The experimental results from helium atom indicate that this mismatch is not so important as it would be expected. Otherwise, no linear dependence of the adsorption energy on the carbon chain length could be observed. In fact, this linear dependence is a clear indication that alkanes adsorb on the Au(111) surfaces with their skeleton planes being parallel to Au(111), since a perpendicular adsorption geometry would lead to an odd/even chain length effect with the methylene group being arranged in the high and low positions above the surface.<sup>[29]</sup>

Since alkanes bind to the surfaces in a flat and all-*trans* conformation, close-packing models of the monolayers can be depicted.<sup>[15,19]</sup> Figure 7a shows the side-by-side packing with a perpendicular boundary. However, two kinds of tilted lamellar structures are possible as shown in Figure 7b and c, which correspond to the neighboring alkane molecules that shift towards the left and right direction, respectively. These

two different types of packing result in the different connection among the terminal methyl groups in the nearest neighboring domains of alkane lamellae. Carefully comparing the schematic packing models to the high-resolution image in Figure 6b, we find that the alkane lamellae adopt the packing structure of Figure 7b. Hence, it is interesting to see that the alkane packing structure becomes chiral on the surface, and we consider the type of packing in Figure 7b to be the unique packing structure in the alkane monolayer on the Au(111) surface.

As described in our previous paper,<sup>[20]</sup> even alkane molecules like  $nC_{36}H_{74}$  form zigzag lamellar rows. Figure 8 presents examples of the zigzag lamellar rows with other alkane molecules such as  $nC_{14}H_{30}$ ,  $nC_{20}H_{42}$ ,  $nC_{26}H_{54}$ , and  $nC_{28}H_{58}$ . Careful inspection of the STM images reveals that the direction of the molecular axis turns at an angle  $\alpha$  as the direction of the lamellar row changes. For  $nC_{14}H_{30}$ , Uosaki et al. reported  $\alpha$  to be about  $12^\circ$ – $15^\circ$ .<sup>[15]</sup> We checked all the alkane lamellae and the measured angles are summarized in

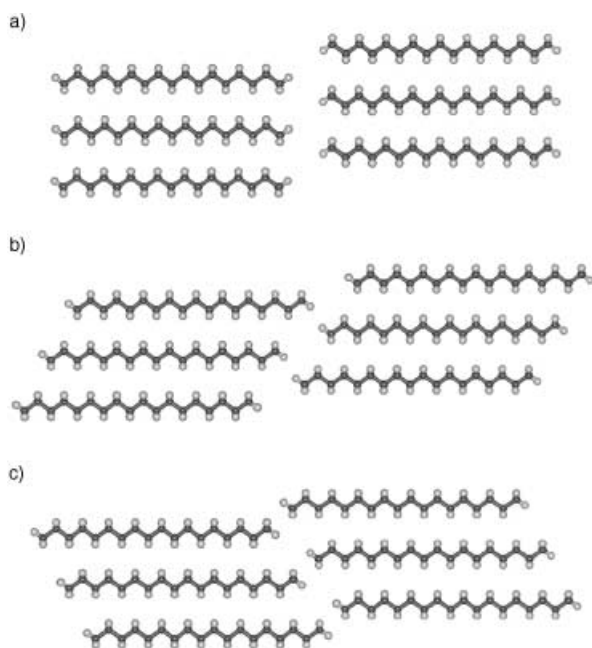


Figure 7. Schematic two-dimensional packing models of even alkanes. a) A perpendicular packing model; b) and c) Two possible tilted packing models.

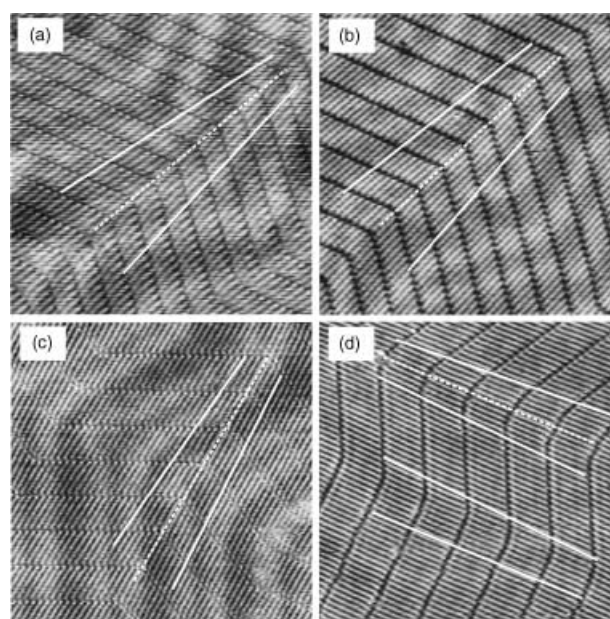


Figure 8. STM images of some even alkanes a)  $C_{14}H_{30}$ , b)  $C_{20}H_{42}$ , c)  $C_{26}H_{54}$  and d)  $C_{28}H_{58}$ , which shows the orientation difference in the adjacent domains of alkane lamellae. All images are of  $25\text{ nm} \times 25\text{ nm}$ .

Table 1. From the data listed in Table 1, it is obvious that angle  $\alpha$  decreases with an increase in carbon chain length.

The STM images reveal that the transition points of the zigzag lamellae are located in a line, which is perpendicular to the direction of gold elbows, as illustrated by the dotted lines in Figure 8. The dotted line bisects angle  $\alpha$  formed by alkane molecules represented by two solid lines on both sides of a lamellar elbow. Notice that for a perpendicular lamella, the long axes of the alkane molecules are parallel to the dotted line, such that orientation change of half  $\alpha$  is experienced when the direction of the lamellar row changes from a tilted lamella to a perpendicular one. Figure 8d presents such an example, in which tilted and perpendicular lamellae coexist for  $n\text{C}_{28}\text{H}_{58}$ . Therefore, we measured that the molecular orientation changes by  $\sim 7.0^\circ$  between two tilted lamellae, and  $\sim 3.5^\circ$  between a tilted lamella and a perpendicular lamella.

The direction of gold elbows is along the  $[11\bar{2}]$  direction, the dotted line perpendicular to  $[11\bar{2}]$  is thus along the  $[01\bar{1}]$  direction (c.f. Figure 2). The observation that the long axes of the alkane molecules would intersect with the dotted line shows that the alkane molecules in a tilted lamella deviate, to a certain extent, from the  $[01\bar{1}]$  direction, whereas the alkane molecules in a perpendicular lamella adsorb along the  $[01\bar{1}]$  direction. Longer chain alkanes form perpendicular lamellae on the reconstructed Au(111) surfaces. As the carbon chain becomes shorter, the alkane–gold interaction becomes weaker. Hence, there is a chance that alkanes confined within the gold troughs migrate along the  $[01\bar{1}]$  direction before becoming desorbed from the surfaces in the case of the alkane–gold interactions become even weaker. This may lead to the formation of a tilted lamella. When the lamellae is tilted, the interaction between the terminal methyl groups of the neighboring lamellae is operative. We infer that it is this interaction that makes the alkane molecules deviate from the  $[01\bar{1}]$  direction.

Based on this assumption, we establish a model for the tilted coterminous lamellae as shown in Figure 9. Although alkane molecules are confined in the gold troughs along the  $[01\bar{1}]$  direction, each molecule turns by a certain angle in order to let the terminal methyl group locate in an optimized position. It is thus anticipated that longer chain alkanes only need to turn a smaller angle than shorter alkanes in order to find the optimal positions for the terminal methyl groups. This correlates well with the observation that angle  $\alpha$  decreases with an increase in the number of carbon atoms in the tilted alkane monolayer. According to the schematic model proposed in Figure 9, the calculated values of

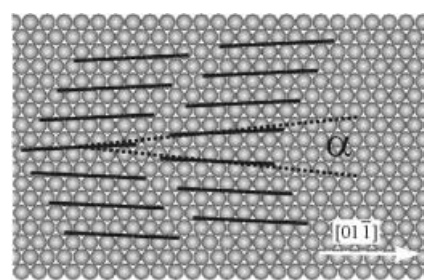


Figure 9. Schematic model of possible arrangement of alkanes on Au(111) surfaces in the coterminous tilted lamellar domains. Each molecule turns a certain angle, but is still confined in the gold trough along the  $[01\bar{1}]$  direction.

angle  $\alpha$  are also listed in Table 1, and are compared with the measured values. Apparently, the agreement between the calculated values and the measured ones is satisfactory, which lends strong support to our model.

There is a dispute on the intermolecular spacing within a lamella. Uosaki et al. reported 0.43 nm for  $n\text{C}_{12}\text{H}_{26}$  and  $n\text{C}_{16}\text{H}_{34}$ , while Cousty et al. reported  $0.5 \pm 0.05$  nm for a normal alkane.<sup>[22]</sup> We advocate 0.48 nm as such a commensurate structure between the alkane monolayer and the reconstructed Au(111) surface is achieved. This is true for odd alkanes and even alkanes of high carbon number ( $n \geq 38$ ), since these alkanes adopt a perpendicular lamellar structure. For even alkane of low carbon number ( $n < 38$ ), the tilted lamellar structure gradually prevails. As alkanes in a tilted lamella deviate from the exact  $[01\bar{1}]$  direction, the intermolecular spacing should be shorter than 0.48 nm. In practice, it is nontrivial to make an accurate measurement of the intermolecular spacing. The model shown in Figure 9 can be used to deduce the theoretical value of the intermolecular spacing for  $n\text{C}_n\text{H}_{2n+2}$  in the tilted lamellae. The obtained data for  $n\text{C}_n\text{H}_{2n+2}$  ( $14 \leq n \leq 28$ ) are listed in the third row of Table 1. We calculated the intermolecular spacing, which changed from 0.45 nm to 0.47 nm as  $n$  changed from 14 to 38. In fact, in the STM image with both perpendicular and tilted lamellae, such as the monolayer of  $n\text{C}_{28}\text{H}_{58}$  (Figure 8d), intermolecular spacing in the tilted lamellae is slightly smaller than that of the perpendicular lamellae. Assuming the intermolecular spacing in the perpendicular lamellae to be 0.48 nm, the intermolecular spacing in the tilted lamellae is calibrated to 0.465 nm in Figure 8d; this is in turn in good agreement to the calculated value.

As discussed above, the packing of the alkanes results in a two-dimensional chiral structure in the tilted alkane lamellae. There should be an equivalent packing structure on the

Table 1. Summary of structural details of the tilted alkane monolayer lamellae on Au (111) surfaces.  $\alpha$  is the angle difference of alkane orientation in the two different tilted lamellar domains as shown in the schematic model of Figure 10.

Normal alkanes	Angle $\alpha$		Calculated Intermolecular distance [nm]
	Calculated [°]	Measured [°]	
$\text{C}_{14}\text{H}_{30}$	13.7	13–14	0.447
$\text{C}_{18}\text{H}_{38}$	11.0	10–11	0.454
$\text{C}_{20}\text{H}_{42}$	10	9–10	0.456
$\text{C}_{22}\text{H}_{46}$	9.1	8–9	0.459
$\text{C}_{24}\text{H}_{50}$	8.4	8–9	0.460
$\text{C}_{26}\text{H}_{54}$	7.8	7–8	0.462
$\text{C}_{28}\text{H}_{58}$	7.3	6–7	0.463

gold surface, which leads to its mirror structure. While the structure and its mirror structure coexist on the surface, zigzag lamellae form, as shown in the proposed model in Figure 9. The angle  $\alpha$  is formed due to alkane molecules in both structures deviating in the opposite direction of the gold troughs. From the high resolution STM image shown in Figure 10, the mirror lamellar structures are confirmed.

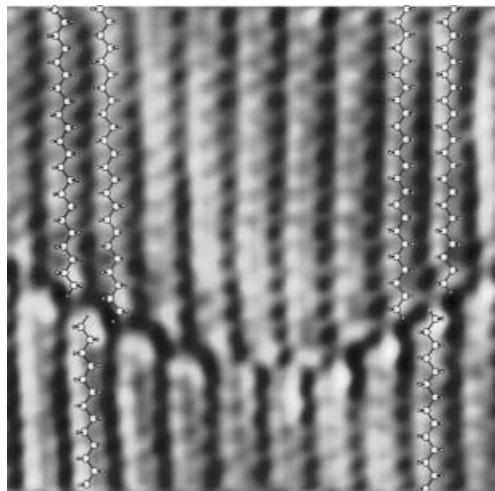


Figure 10. STM image of atomic resolution for  $n\text{C}_{28}\text{H}_{58}$  at the boundary of two tilted lamellar domains, showing the mirror structures.

## Conclusion

We performed a systematic STM study on the self-assembled monolayers of alkane molecules with different carbon chain lengths (from  $\text{C}_{14}\text{H}_{30}$  to  $\text{C}_{38}\text{H}_{78}$ ) on reconstructed Au(111) surfaces. Despite the fact earlier studies concluded that some  $n$ -alkanes (from  $n=18$  to  $n=26$ ) cannot form well-ordered structures on Au (111) surfaces,<sup>[17,21,22]</sup> we successfully observed well-ordered monolayers of these alkanes. We propose a structural model for the packing of alkane molecules on reconstructed Au (111) surfaces, which successfully explains the experimental observations. Our main conclusions are:

- 1) Alkanes lie flat on gold surfaces. The gold reconstruction plays a critical role in the formation of the well-ordered monolayers. The self-assembled structures of normal alkanes are commensurate with the reconstructed Au (111) surfaces, in which alkane molecules pack side-by-side with alkanes adsorbed in the gold troughs along the  $[01\bar{1}]$  direction.
- 2) At room temperature ( $25^\circ\text{C}$ ), tilted lamellae form if  $n < 22$ , tilted and perpendicular lamellae coexist for  $36 \geq n \geq 22$ , and perpendicular lamellae prevail for  $n \geq 38$ . The observed lamellar structures are determined by a combined effect of the adsorbate–adsorbate interactions and the adsorbate–substrate interactions. A strong adsorbate–substrate interaction favors the perpendicular lamellae, while a tilted lamella is preferable if the adsorbate–substrate interaction is weak.

- 3) In the tilted lamellae, the interactions between the terminal methyl groups of the neighboring lamellae make the alkane molecules deviate from the  $[01\bar{1}]$  direction, which in turn, leads to an intermolecular spacing smaller than the commensurate periodicity 0.48 nm. The deviation angle  $\alpha$  decreases with an increase in the carbon number.
- 4) A two-dimensional chiral structure forms in the tilted alkane-lamellae, which results in the angle difference of molecular orientation in the zigzag alkane lamellae.

## Acknowledgement

This work was supported by the National Natural Science Foundation of China (Grant No. 20021002, 20173046), the Ministry of Science and Technology of China (No. 2001CB610506), and TRAPOYT from the Ministry of Education of China.

- [1] S. Hoepfner, L. F. Chi, H. Fuchs, *Nano Lett.* **2002**, *2*, 459–463.
- [2] L. E. Firment, G. A. Somorjai, *J. Chem. Phys.* **1977**, *66*, 2901–2913.
- [3] L. E. Firment, G. A. Somorjai, *J. Chem. Phys.* **1978**, *69*, 3940–3952.
- [4] M. Yamamoto, Y. Sakurai, Y. Hosoi, H. Ishii, E. Ito, K. Kajikawa, Y. Ouchi, K. Seki, *J. Phys. Chem. B* **2000**, *104*, 7363–7369.
- [5] J. S. Foster, J. E. Frommer, *Nature* **1988**, *333*, 542–545.
- [6] D. P. E. Smith, H. Horber, Ch. Gerber, G. Binnig, *Science* **1989**, *245*, 43–45.
- [7] J. P. Rabe, S. Buchholz, *Science* **1991**, *253*, 424–427.
- [8] A. Ikai, *Surf. Sci. Rep.* **1996**, *26*, 263–332.
- [9] L. C. Giancarlo, G. W. Flynn, *Annu. Rev. Phys. Chem.* **1998**, *49*, 297–336.
- [10] S. Cincotti, J. P. Rabe, *Appl. Phys. Lett.* **1993**, *62*, 3531–3533.
- [11] L. C. Giancarlo, H. Fang, S. M. Rubin, A. A. Bront, G. W. Flynn, *J. Phys. Chem. B* **1998**, *102*, 10255–10263.
- [12] T. K. Xia, U. Landman, *Science* **1993**, *261*, 1310–1312.
- [13] T. K. Xia, U. Landman, *Phys. Rev. B* **1993**, *48*, 11313–11316.
- [14] K. Uosaki, R. Yamada, *J. Am. Chem. Soc.* **1999**, *121*, 4090–4091.
- [15] R. Yamada, K. Uosaki, *J. Phys. Chem. B* **2000**, *104*, 6021–6027.
- [16] Z. X. Xie, X. Xu, J. Tang, B. W. Mao, *J. Phys. Chem. B* **2000**, *104*, 11719–11722.
- [17] O. Marchenko, J. Cousty, *Phys. Rev. Lett.* **2000**, *84*, 5363–5366.
- [18] R. Yamada, K. Uosaki, *Langmuir* **2000**, *16*, 4413–4415.
- [19] Z. X. Xie, X. Xu, J. Tang, B. W. Mao, *Chem. Phys. Lett.* **2000**, *323*, 209–216.
- [20] Z. X. Xie, Z. F. Huang, X. Xu, *Phys. Chem. Chem. Phys.* **2002**, *4*, 1486–1489.
- [21] A. Marchenko, J. Cousty, L. P. Van, *Langmuir* **2002**, *18*, 1171–1175.
- [22] J. Cousty, A. Marchenko, *Surf. Sci.* **2002**, *520*, 128–136.
- [23] Y. F. He, T. Ye, E. Borguet, *J. Phys. Chem. B* **2002**, *106*, 11264–11271.
- [24] J. Clavilier, *J. Electroanal. Chem.* **1980**, *107*, 211–216.
- [25] Z. X. Xie, X. Xu, B. W. Mao, K. Tanaka, *Langmuir* **2002**, *18*, 3113–3116.
- [26] Ch. Wöll, S. Chiang, R. J. Wilson, P. H. Lippel, *Phys. Rev. B* **1989**, *39*, 7988–7991.
- [27] S. Cincotti, J. Burda, R. Hentschke, J. P. Rabe, *Phys. Rev. E* **1995**, *51*, 2090–2098.
- [28] A. J. Groszek, *Nature* **1964**, *204*, 680–681.
- [29] S. M. Wetterer, D. J. Lavrich, T. Cummings, S. L. Bernasek, G. Scoles, *J. Phys. Chem.* **1998**, *102*, 9266–9275.
- [30] K. R. Paserba, A. J. Gellman, *J. Chem. Phys.* **2001**, *115*, 6737–6751.

Received: July 14, 2003

Revised: October 29, 2003 [F5334]